Am J Transl Res 2021;13(4):3906-3916
www.ajtr.org /ISSN:1943-8141/AJTR0111988

Original Article

Knockdown of lncRNA RMST protect against myocardial infarction through regulating miR-5692 and MAGI3 axis

Qiaoling Zhang, Famin Ye, Suping Guo, Wentao Xiao, Jingjing Zhang, Yongsheng Qu, Jing Zhang

Heart Center of Henan Provincial People's Hospital, Central China Fuwai Hospital, Central China Fuwai Hospital of Zhengzhou University, Zhengzhou, Henan, China

Received April 5, 2020; Accepted December 11, 2020; Epub April 15, 2021; Published April 30, 2021

Abstract: Aims: Myocardial infarction is the leading cause of death worldwide. The aim of this study was to investigate the function and mechanism of lncRNA RMST in myocardial infarction. Materials and methods: H/R and H_2O_2 models were established to assess the function of lncRNA RMST in vitro. Mouse myocardial infarction was used to analyze the function of lncRNA RMST in vivo. Bioinformatics analysis was performed to predict the potential binding target of lncRNA RMST. Rescue experiments were performed to verify the relationship between RMST and its target. Results: The expression of lncRNA RMST was significantly increased with H/R or H_2O_2 treatment. Knockdown of lncRNA RMST improved cell death and protected mitochondria from H/R injury in vitro. In vivo, cardiac function was significantly attenuated by knockdown of lncRNA RMST. We also provided evidence that miR-5692 was a direct target of lncRNA RMST. Rescue experiments showed that knockdown of miR-5692 could restore the function of RMST. Conclusion: Our study is the first to prove the function and mechanism of lncRNA RMST in myocardial infarction. Thus, a deeper understanding of the role of lncRNA RMST in myocardial infarction may provide new insights for the clinical intervention of MI.

Keywords: Myocardial infarction, lncRNA, target, RMST, H/R

Introduction

Acute myocardial infarction (AMI) is one of the most serious cardiovascular diseases [1] characterized by coronary artery occlusion [2] and myocardial cell necrosis and is the leading cause of death worldwide [3, 4]. Numerous studies have shown that sudden reopening of the occluded coronary artery and restoration of blood flow in AMI patients could cause dysfunction of vascular endothelial cells [5] and activation of related inflammatory factors [6], which aggravate myocardial cell injury after ischemia/reperfusion (I/R). Previous studies have also indicated that approximately 40% of cell damage during revascularization after AMI is caused by reperfusion injury [7, 8]. Therefore, reducing I/R damage plays a very important role in the treatment of AMI.

Long noncoding RNA is a type of RNA without protein-coding potential [9]. Numerous studies have revealed the different roles of lncRNAs in pathological processes, including diabetes [10], heart diseases [11], tumors [12] and other diseases [13]. The functions of lncRNAs can also vary, including chromatin remodeling [14], transcriptional regulation [15] and posttranslational regulation [16]. Increasing evidence has revealed that mutations and dysregulations of lncRNAs are tightly associated with several human diseases ranging from cardiovascular diseases to many cancers. For example, lncRNA Gm2691 improved cardiac function and cell viability by regulating the Akt signaling pathway [17]. Overexpression of lncRNA uc.4 can inhibit cell differentiation by regulating the TGF-b signaling pathway [18]. Thus, further research on the roles of lncRNAs in cardiovascular disease will deepen our understanding of the pathological process of this disease.

The lncRNA RMST has been shown to play an important role in cerebral ischemic disease [19, 20]. Knockdown of RMST prevents neuronal differentiation, suggesting a critical role in neuronal differentiation [21]. Previous studies have shown that RMST silencing protects against

ischemic brain injury in vivo and neuron injury in vitro [22]. RMST silencing could reduce ischemia-induced brain infarct size and improve neurological function. However, the function of RMST in cardiovascular disease remains unknown.

In this study, we aimed to investigate the function and mechanism of lncRNA RMST in myocardial infarction. Apoptosis, LDH and death rates were determined to analyze the function of RMST in vitro. Cardiac function and cardiac markers were assessed to determine the function of RMST in vivo. Additionally, we predicted the potential binding target of RMST and performed rescue experiments. Our results showed that the expression of lncRNA RMST was significantly increased under H/R or H_2O_2 treatment. Knockdown of lncRNA RMST improved cell death and protected mitochondria from H/R injury in vitro. In an in vivo study, cardiac function was significantly attenuated by knockdown of lncRNA RMST. We also provided evidence that miR-5692 was the direct target of lncRNA RMST. Rescue experiments showed that knockdown of miR-5692 could restore the function of RMST. Our study was the first to prove the function and mechanism of lncRNA RMST in myocardial infarction. Thus, a deeper understanding of the role of lncRNA RMST in myocardial infarction may provide new insights for the clinical intervention of MI.

Materials and methods

Cell culture

Cells were grown at 5% CO_2 with Dulbecco's modified Eagle's medium (DMEM) containing 10% fetal bovine serum (FBS Invitrogen, Gibco) and 100 mg/ml penicillin/streptomycin. To mimic hypoxia reperfusion injury, NRVMs were first washed twice with PBS and then incubated with I/R buffer (4 mM HEPES, 117 mM NaCl, 12 mM KCl, 0.9 mM $CaCl_2$, 0.49 mM $MgCl_2$, 20 mM sodium lactate, 5.6 mM 2-deoxy-glucose, pH 6.2). NRVMs were then placed in a hypoxia chamber (Billups-Rothenberg) and flushed with 95% N_2/5% CO_2 for 30 min. The cells were then treated in serum-free DMEM with 300 μM H_2O_2 for 2 hours in a 5% CO_2 incubator at 37°C.

Death rates

Trypan blue staining (Beyotime, China) was used to calculate the mortality of primary cardiomyocytes. In H/R model, cells were digested after 12 h reperfusion. Trypan blue was used to stain the cells, and measurements were taken according to the manufacturer's instructions.

LDH release

Levels of released lactate dehydrogenase (LDH) were detected in serum using an LDH release assay kit (Beyotime, China) according to the manufacturer's protocol.

Western blot

Cardiomyocytes were lysed for 30 min on ice with RIPA lysis buffer (Solarbio, Beijing, China) containing 0.1 mM PMSF and a protease inhibitor (Roche), and the BCA protein assay kit (Beyotime, Nantong, China) was used to detect the protein concentrations. Primary antibodies against Bax, Bcl-2, HSP90 and MAGI3 were all obtained from Cell Signaling Technology (Beverly, USA), and HSP90 was used as a loading control.

PCR

Total RNA from NRVMs was extracted using TRIzol (Invitrogen), and cDNA was synthesized using an iScript cDNA Synthesis Kit (Bio-Rad, Hercules, CA). An ABI Prism 7900 Sequence Detection System (Applied Biosystems) was used to perform quantitative real-time PCR (qRT-PCR). ANP forward primer, 5'-GAACCTGCTAGACCACCT; reverse primer, 5'-CCTAGTCCACTCTGGGCT. BNP forward primer, 5'-AAGCTGCTGGAGCTGATAAGA; reverse primer, 5'-GTTACAGCCCAAACGACTGAC. GAPDH was used as an internal normalization reference for RMST and other genes. The $2^{-\Delta\Delta Ct}$ method was used to calculate gene expression levels.

Hoechst staining

Briefly, cells were seeded on sterile cover glasses placed in 6-well plates the day before treatment. Then, the cells were fixed, washed twice with PBS and stained with Hoechst 33258 (Apoptosis Hoechst staining kit, Beyotime Biotechnology, Shanghai, China) according to the manufacturer's instructions. The stained cells were examined and immediately imaged under a fluorescence microscope (Nikon, Japan). At least 3 visual fields were chosen for analysis. The rate of apoptotic cell nuclei is defined as apoptotic positive cell nuclei/total

cell nuclei in the field. The fluorescence of the cells was detected and quantified by ImageJ software.

I/R cardiac animal model

The male C57BL/6J mice (6-10 weeks of age, 20~22 g) used in our study were obtained from the Animal Research Center of Henan Provincial People Hospital, and the study was approved by the Animal Nursing Committee of Henan Provincial People Hospital. A total of 30 mice were used, of which 6 were used as controls, and the remaining 24 underwent I/R surgery. In the I/R process, the left anterior descending branch (LAD) was occluded for 60 min and then reperfused for 1 week. After 1 week of reperfusion injury, the mice were sacrificed for further analysis. Mouse after reperfusion injury were sacrificed and heart tissues were harvested for ANP and BNP measurement.

Echocardiography analysis

Echocardiography was used to evaluate cardiac function in mice. In the I/R operation, the ST segment elevation and QRS wave width were used to confirm ischemia. At the end of the animal experiment, the LV ejection fraction (EF) and fractional shortening rate (FS) were calculated. M-mode recordings at the level of the papillary muscles were conducted to measure systolic and diastolic left ventricular internal dimensions. Fractional shorting was calculated as (LVIDd-LVIDs)/LVIDd and expressed as percentage.

Dual-luciferase reporter assay

RMST with wild-type or mutant (mut) binding sites for miR-5692a was amplified and cloned into the pGL3 vector (Promega, Madison, WI, USA). HEK 293 cells were used to perform the luciferase reporter assay, and the miR-5692a mimics and RMST vector were cotransfected using Lipofectamine 3000 reagent. Luciferase activity was analyzed using a dual-luciferase system following the manufacturer's protocol.

RIP

RIP experiments were conducted using the Magna RIP RNA-Binding Protein Immunoprecipitation kit (Catalog No. 17-700, Millipore). Cardiomyocytes were lysed, and the whole cell lysates were cultured with protein magnetic beads, which were conjugated using 2 μg of MAGI3 antibody or control IgG at 4°C overnight. The immunoprecipitated RNA was purified and analyzed by RT-qPCR.

Statistical analysis

All results are expressed as the mean ± SD. Student's t-tests were used to determine significant differences. Comparisons between groups were performed by one-way analysis of variance (ANOVA), and p values < 0.05 (*) and 0.01 (**) were considered significant.

Results

LncRNA RMST was increased under H/R and H_2O_2 conditions

To investigate the function of RMST, we first established H/R and H_2O_2 models. After 5 hours of hypoxia, cardiomyocytes were recultured in normal culture medium overnight. Our results showed that death rates were significantly increased after H/R treatment. We also assessed the death rates when cells were treated with 300 μm H_2O_2 for 2 hours. H_2O_2 also increased the cell death rates (**Figure 1A**). In addition, we measured LDH release and found that the H/R and H_2O_2 models increased LDH levels (**Figure 1B**). LncRNA RMST was mainly located in the cytoplasm, as indicated in the cytoplasm and nucleus isloation experiment (**Figure 1C**). Finally, we detected the expression of RMST in the H/R and H_2O_2 models, and found that it was significantly increased compared with that in the control group (**Figure 1D**). Thus, our results suggest that lncRNA RMST may play a role in H/R injury.

Functional analysis of RMST in vitro

To explore the function of RMST, we first knocked down the lncRNA and verified the knockdown efficiency. PCR results showed that lncRNA RMST was knocked down by 80% (**Figure 2A**). Next, we performed a comprehensive analysis of lncRNA RMST in vitro. Knockdown of lncRNA RMST significantly reduced cell injury, as evidenced by a reduction in cell death rates and LDH release (**Figure 2B**, **2C**). We also assessed the cell apoptosis markers Bax and Bcl-2 by western blotting. Knockdown of lncRNA RMST significantly reduced cell apop-

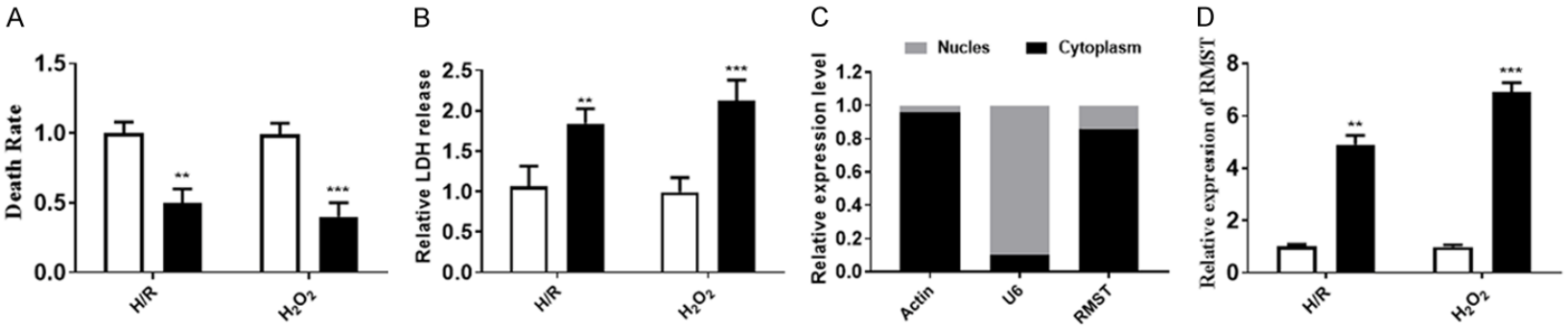

Figure 1. LncRNA RMST was upregulated exposed to H/R and H_2O_2. A. Death rates were downregulated exposed to H/R and H_2O_2. B. LDH release was upregulated exposed to H/R and H_2O_2. C. RMST was mainly located in cytoplasm. D. The expression of lncRNA RMST was upregulated exposed to H/R and H_2O_2.

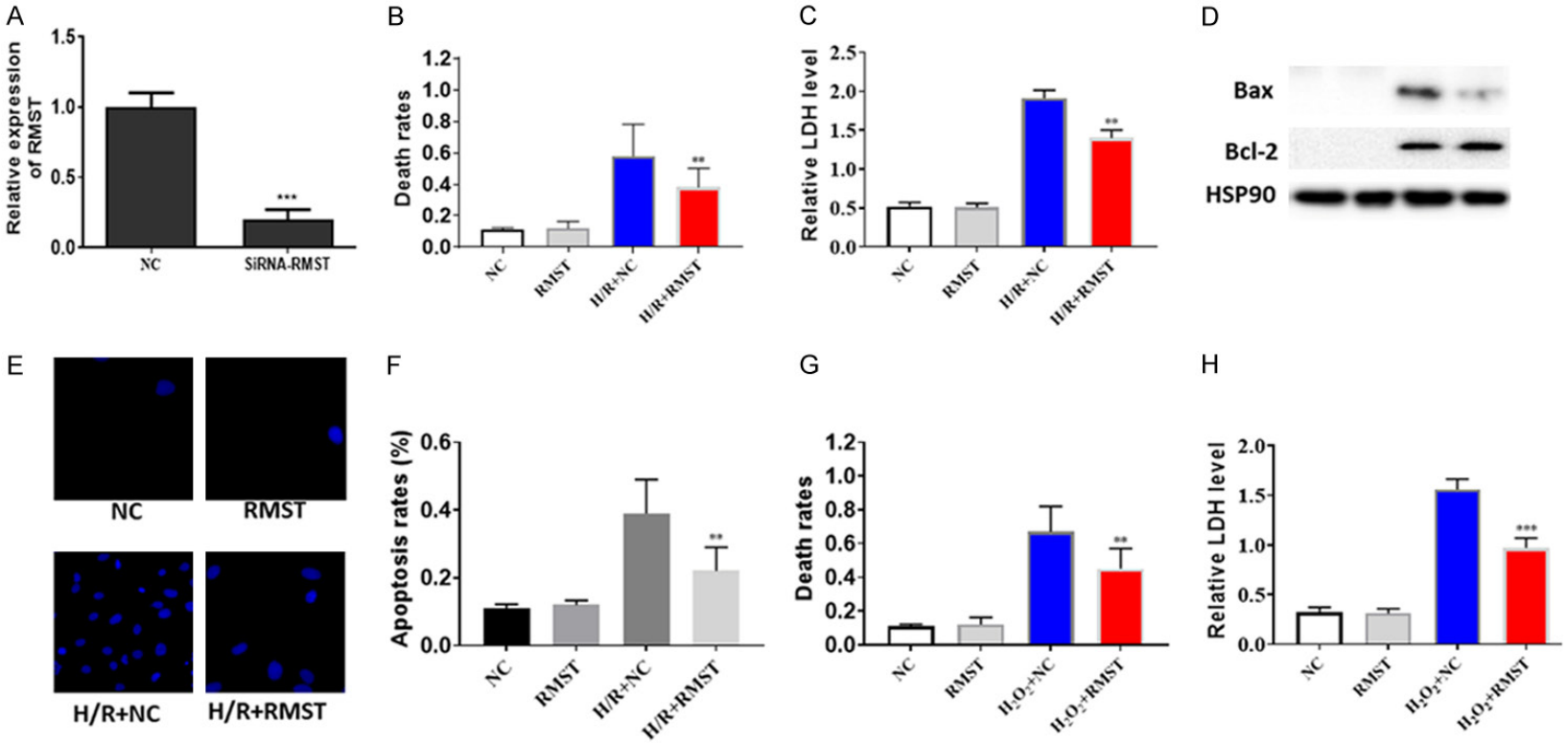

Figure 2. Function analysis of lncRNA RMST in cardiomyocytes. A. Knockdown of RMST was verified. B. Knockdown of RMST reduced the cell death rates in H/R. C. LDH release was increased in knockdown of RMST in H/R. D. Apoptosis markers were detected via western blot. E. Hoechst staining was performed to detect the apoptosis. F. Quantification data was measured. G. Death rates were reduced in knockdown of RMST in H_2O_2 model. H. Knockdown of RMST reduced the LDH release in H_2O_2 model.

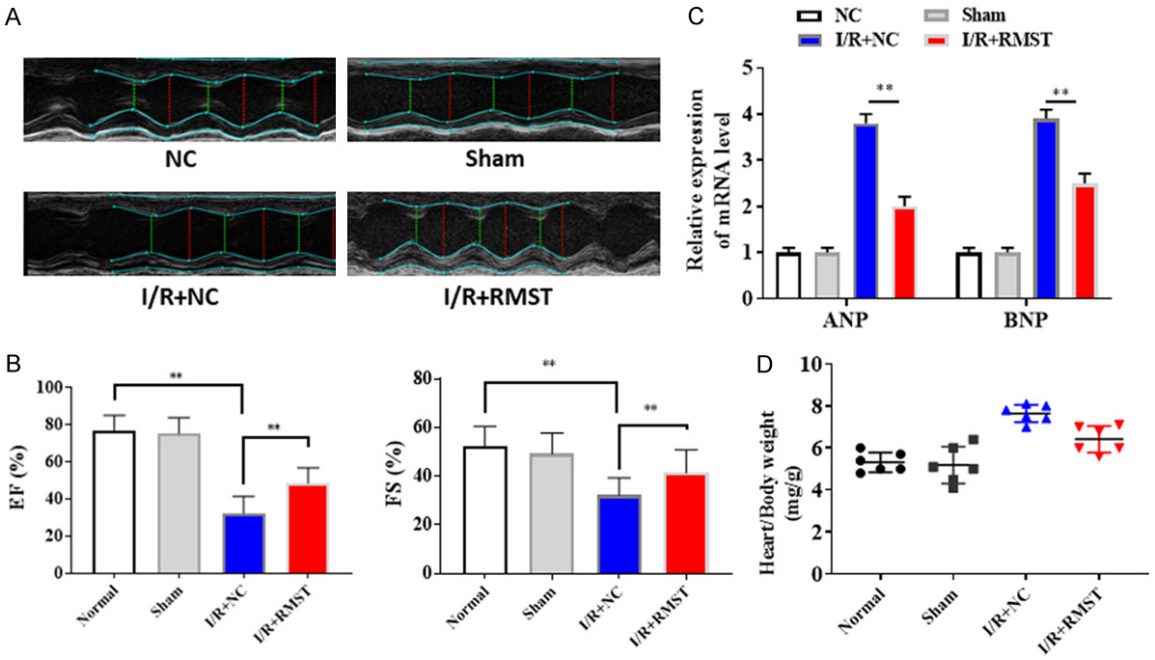

Figure 3. Function of RMST in vivo. A. Echocardiography analysis was recorded. B. EF and FS were measured. (N=6 per group, one-way ANOVA analysis with Bonferroni's multiple comparison test). C. Cardiac markers ANP and BNP were measured via real-time PCR. (N=6 per group, one-way ANOVA analysis with Bonferroni's multiple comparison test). D. Heart weight and body weight were recorded. (N=6 per group, one-way ANOVA analysis with Bonferroni's multiple comparison test).

tosis, as indicated by decreased Bax expression and increased Bcl-2 expression (**Figure 2D**). We also performed Hoechst staining, which demonstrated that knockdown of lncRNA RMST effectively reduced the cell apoptosis rates in the H/R model (**Figure 2E**, **2F**). In addition, we also examined the function of RMST in the H_2O_2 model. Knockdown of lncRNA RMST protected cardiomyocytes against the cell injury induced by the H_2O_2 model, as evidenced by a decrease in cell death rates and LDH release (**Figure 2G**, **2H**). Thus, our results suggest that knockdown of lncRNA RMST protects cells from ischemic reperfusion injury.

Functional analysis of RMST in vivo

To further explore the function of RMST in vivo, we established an MI animal model. After 1 hour of ligation, the mice were maintained for 1 week of reperfusion and then sacrificed for further analysis. Echocardiography was used to record cardiac remodeling. Knockdown of lncRNA RMST significantly improved cardiac function, as evidenced by improved EF and FS (**Figure 3A**, **3B**). We also measured the cardiac markers ANP and BNP, which were significantly downregulated after knockdown of lncRNA RMST (**Figure 3C**). Finally, we measured the heart weight and body weight. Knockdown of lncRNA RMST clearly reduced this ratio, suggesting a protective role for lncRNA RMST in myocardial infarction (**Figure 3D**).

miR-5692a is a direct target of RMST

To investigate the possible mechanism involving RMST, first we used bioinformatic analysis to predict the potential binding target. Considering the location of this lncRNA, we predicted the miRNAs that it may bind to, among which miR-5692a had the highest fold change. The

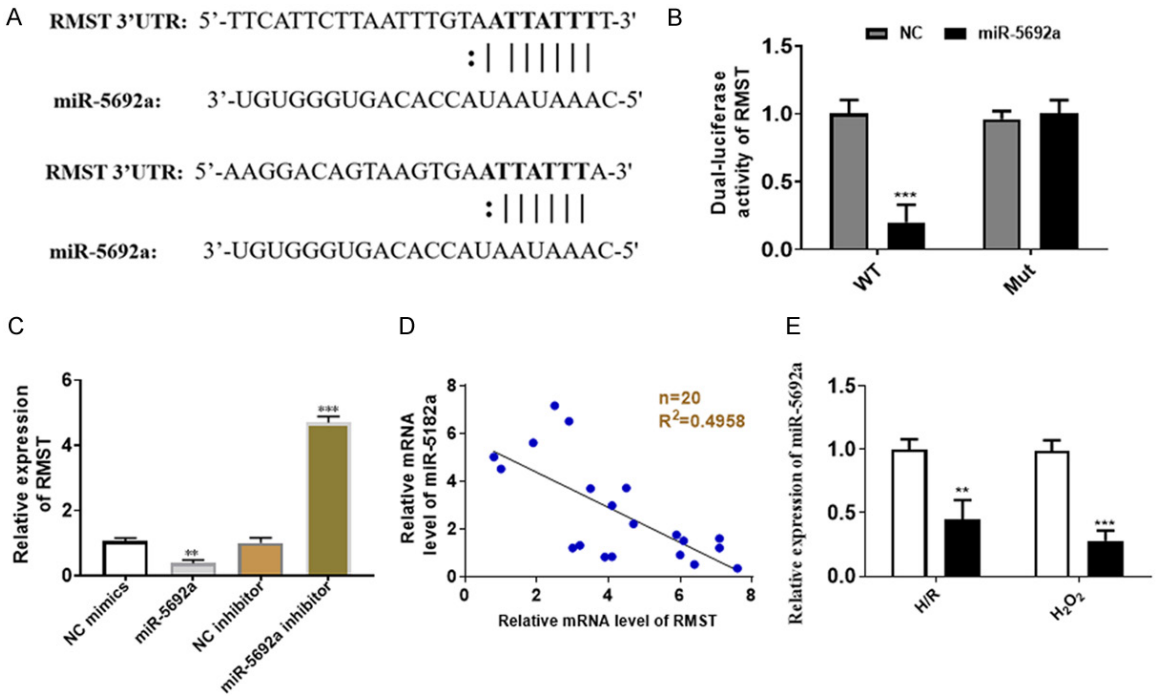

Figure 4. miR-5692a is the direct target of RMST. A. The potential binding sequence was showed. B. Dual-luciferase reporter assay was detected to verify the relationship between miR-5692a and RMST. C. miR-5692a negatively regulate expression of RMST. D. miR-5692a negatively regulate the expression of RMST. E. The expression of miR-5692a was significantly downregulated in H/R and H_2O_2 model.

potential binding sequences are shown in **Figure 4A**. Next, we analyzed the binding relationship between miR-5692a and RMST using a dual-luciferase reporter assay. The relative luciferase activity of the RMST reporter was significantly reduced in the miR-5692a group, whereas no difference was detected in the mutant group (**Figure 4B**). Overexpression of miR-5692a significantly reduced the expression of RMST and knockdown of miR-5692a increased the expression of RMST, suggesting that miR-5692a negatively regulates the expression of RMST (**Figure 4C**, **4D**). Finally, we examined the expression of miR-5692a in the H/R and H_2O_2 models, and our results showed that the expression of miR-5692a was significantly decreased upon H/R and H_2O_2 treatment (**Figure 4E**). Thus, our results suggest that miR-5692a is a direct target of RMST and negatively regulates RMST.

MAGI3 is a direct target of miR-5692a

Here, we used bioinformatics analysis to predict the downstream target of miR-5692a and identified a potential binding site between miR-5692a and MAGI3 (**Figure 5A**). A dual-luciferase reporter assay showed that the relative luciferase activity of the MAGI3 reporter was markedly reduced in the miR-5692a group, whereas no difference was detected in the mutant group (**Figure 5B**). Overexpression of miR-5692a significantly reduced the expression of MAGI3 and the opposite was observed when miR-5629a was knocked down, as demonstrated by real-time PCR (**Figure 5C**). Similar results were observed by western blotting, suggesting that miR-5692a can negatively regulate the expression of MAGI3 (**Figure 5D**). In addition, we also assessed the expression of MAGI3 upon H/R and H_2O_2 treatment. Our results suggested that the expression of MAGI3 was clearly increased upon H/R and H_2O_2 treatment (**Figure 5E**). Finally, we verified the relationship between lncRNA RMST, miR-5692a and MAGI3. RIP experiments showed that lncRNA RMST can bind with miR-5692a (**Figure 5F**). Thus, our results proved that MAGI3 is a direct target of miR-5692a.

The RMST/miR-5692a/MAGI3 axis in MI

To prove the relationship between the factors in the RMST/miR-5692a/MAGI3 axis in MI, we

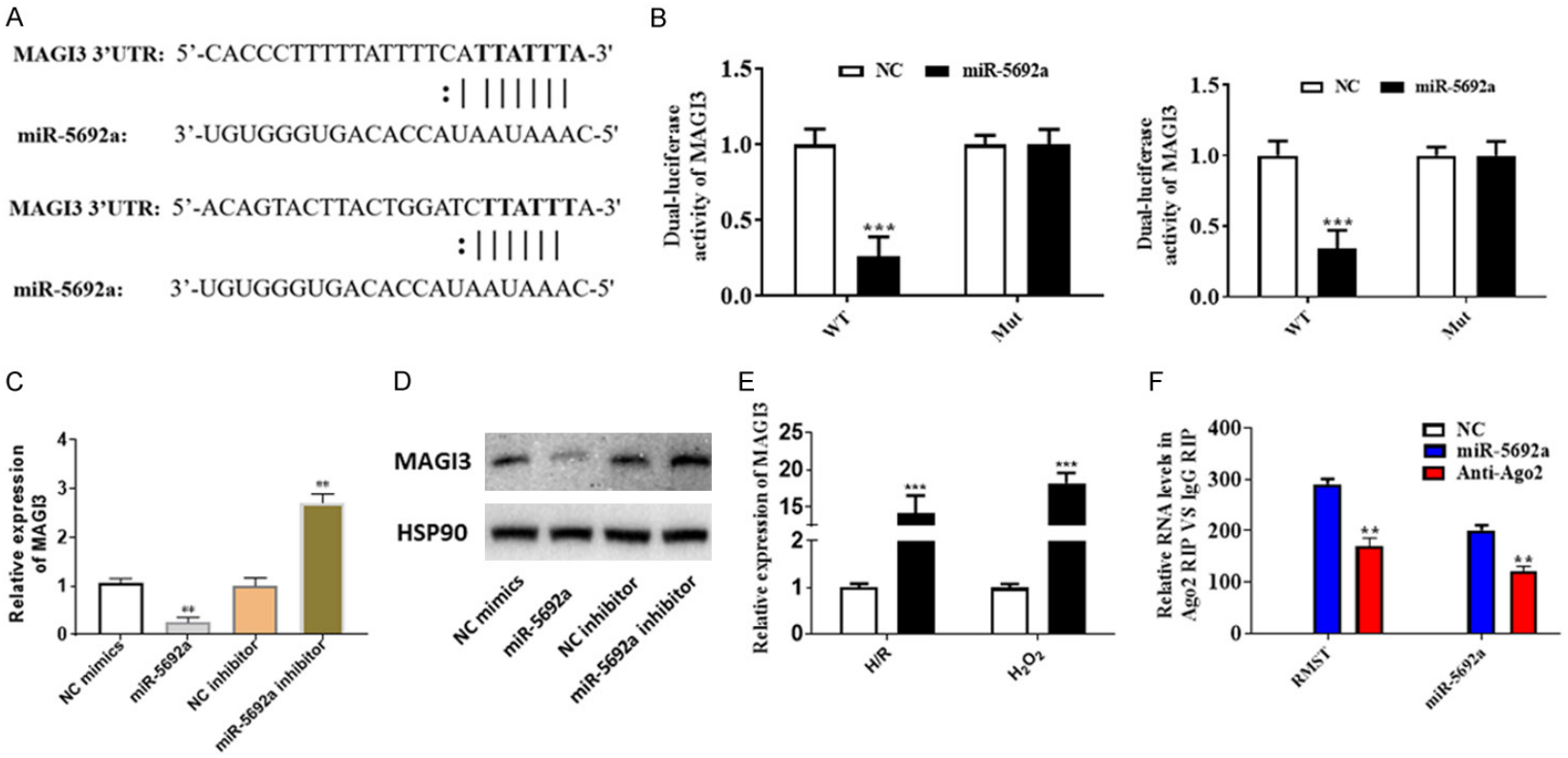

Figure 5. MAGI3 is the direct target of miR-5692a. A. The potential binding sequence between miR-5692a and MAGI3 was showed. B. Dual-luciferase reporter assay was performed to detect the relationship between miR-5692a and MAGI3. C. miR-5692a negatively regulate the expression of MAGI3 via real-time PCR. D. miR-5692a negatively regulate the expression of MAGI3 via western blot. E. The expression of MAGI3 was significantly increased in H/R and H_2O_2 model. F. RIP experiment was performed to verify the binding relationship.

performed a comprehensive rescue experiment. First, knockdown of RMST significantly reduced the expression of MAGI3, as evidenced by a decrease in MAGI3 determined by real-time PCR and western blot (**Figure 6A**, **6B**). Knockdown of miR-5692a partially blocked the effect of lncRNA RMST, as evidenced by increased levels of MAGI3 determined by real-time PCR and western blot (**Figure 6C**, **6D**). Next, a rescue experiment was performed to identify the relationship between RMST and miR-5692a. In the H/R model, knockdown of RMST reduced the cell death rates; however, knockdown of miR-5692a rescued this effect, as indicated by a small increase in death rates (**Figure 6E**). We also analyzed LDH release and found that knockdown of miR-5692a rescued the effect caused by the knockdown of lncRNA RMST (**Figure 6F**). Finally, we detected the apoptosis rates using Hoechst staining and quantified the data. Knockdown of RMST significantly reduced cell apoptosis, and knockdown of miR-5692a restored the anti-apoptotic effect (**Figure 6G**). Thus, our results suggest that lncRNA RMST has a protective function in myocardial infarction by regulating miR-5692a and MAGI3.

Discussion

In this study, we performed a comprehensive functional analysis of lncRNA RMST in myocardial infarction and provided evidence that lncRNA RMST protects against cardiomyocyte injury by regulating miR-5692a and MAGI3. Our study verified this function in different cell models and an animal model. Finally, rescue experiments proved the relationship between miR-5692a and RMST. Our study provides new clues for understanding the mechanism of myocardial infarction.

Reperfusion therapy as soon as possible after AMI can alleviate myocardial ischemia injury [23], but sometimes reperfusion can also aggravate the cardiac dysfunction and structural damage of myocardial cells [24]. This pathological process involves many different pathological reactions, including ROS production [25], inflammation [26], apoptosis [27] and oxidative stress [28]. Apoptosis and death of cardiomyocytes were significantly increased during I/R injury of AMI. Thus, targeting cell death may provide new clues for clinical intervention. H/R and H_2O_2 are commonly used model to study the ischemia injury. Hypoxia and reperfusion model were used to study the ischemia and reperfusion injury, whereas H_2O_2 model was used to analyze the ROS and mitochondrial function. It is essential to demonstrate the potential molecular mechanisms and identify useful therapeutic targets. In the current study, we found that knockdown of RMST decreased the protein level of Bax. Hoechst staining also showed decreased cell apoptosis rates. Thus, our study provides a new target for clinical intervention.

The mechanism of lncRNAs mainly depends on their location [29, 30]. Nuclear lncRNAs can regulate target gene transcription [31, 32]. However, cytoplasmic lncRNAs can act as a sponge to bind miRNAs and thus regulate their target genes. For example, lncRNA RPL34-AS1 inhibits papillary thyroid cancer development by competitively binding miR-3663-3p/RGS4 [33]. Silencing of lncRNA Gm11974 protects against cerebral ischemic reperfusion through the miR-766-3p/NR3C2 axis [34]. Our study predicted the potential binding target of RMST, among which miR-5692a had the highest fold change. Thus, we used a dual-luciferase reporter assay to verify the relationship between the two genes. MicroRNA is also a member of the noncoding RNA family and can bind to the 3'UTR of target mRNA to regulate different cell activities [35]. Previous studies have shown that miR-5692a can promote hepatocellular carcinoma by regulating HOXD8 [36], suggesting that miR-5692a may function in pathological processes. To date, there is no report about the function of miR-5692a in myocardial infarction. Thus, we analyzed the expression of miR-5692a, and the results demonstrated that miR-5692 was downregulated upon H/R and H_2O_2 treatment. In the current study, bioinformatics analysis showed that MAGI3 is a direct target of miR-5692a, and we also provided evidence about their interaction by dual-luciferase reporter assays. MiR-5692a could negatively regulate the expression of MAGI3, and RIP experiments further confirmed the interaction between RMST and miR-5692a. Overall, we proved that lncRNA RMST can sponge miR-5692a and target MAGI3.

Taken together, our findings provide functional data and the mechanism of RMST involvement

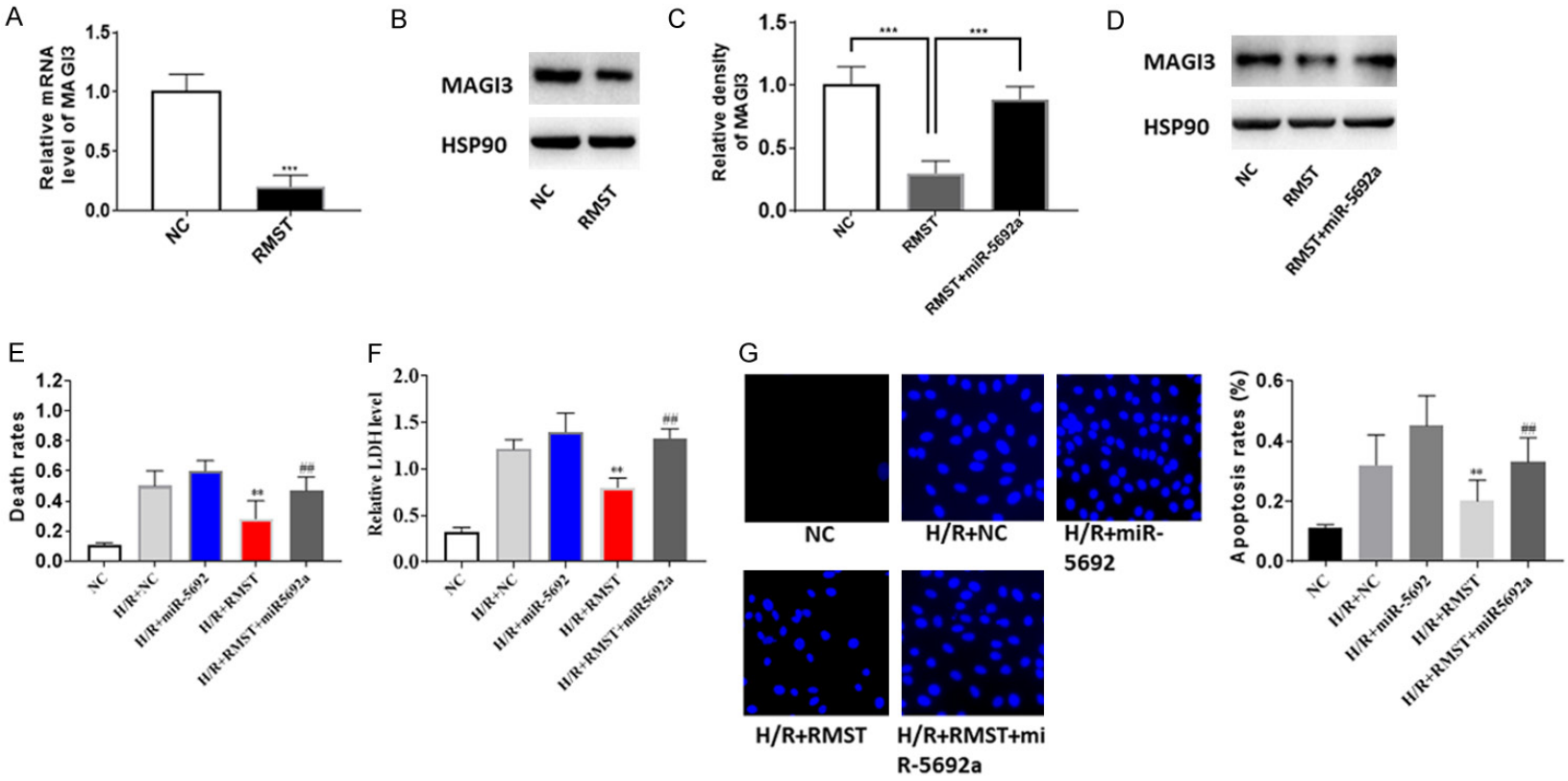

Figure 6. RMST/miR-5692a/MAGI3 pathway in I/R injury. A. Knockdown of RMST significantly reduced the expression of MAGI3 via real-time PCR. B. Knockdown of RMST significantly reduced the expression of MAGI3 via western blot. C. knockdown of miR-5692a blocked the effect of RMST via real-time PCR. D. knockdown of miR-5692a blocked the effect of RMST via western blot. E. Knockdown of miR-5692a rescued the death rates effect induced by knockdown of RMST. F. Knockdown of miR-5692a restored the LDH release of RMST. G. Apoptosis revealed that knockdown of miR-5692a rescued the effect of RMST.

in myocardial infarction. Knockdown of lncRNA RMST improved cell death and protected mitochondria from H/R injury in vitro. In an in vivo study, cardiac function was significantly attenuated by knockdown of lncRNA RMST. We also provided evidence that miR-5692 was the direct target of lncRNA RMST. Rescue experiments showed that overexpression of miR-5692 could restore the function of RMST. Our study is the first to prove the function and mechanism of lncRNA RMST in myocardial infarction. Thus, a deeper understanding of lncRNA RMST in myocardial infarction may provide new insights for the clinical intervention of MI.

Acknowledgements

This work was supported by Scientific and technological research project of Henan Provincial Health Commission (NO. YKL-40).

Disclosure of conflict of interest

None.

Address correspondence to: Jing Zhang, Heart Center of Henan Provincial People's Hospital, Central China Fuwai Hospital, Central China Fuwai Hospital of Zhengzhou University, NO. 1 Fuwai Avenue, Zhengdong New District, Zhengzhou 450000, Henan Province, China. Tel: +86-13703921930; E-mail: zhangjingxnk@aliyun.com

References

[1] Ko DT, Khera R, Lau G, Qiu F, Wang Y, Austin PC, Koh M, Lin Z, Lee DS, Wijeysundera HC and Krumholz HM. Readmission and mortality after hospitalization for myocardial infarction and heart failure. J Am Coll Cardiol 2020; 75: 736-746.

[2] Ghaleb B, Thireau J, Cazorla O, Soleti R, Scheuermann V, Bizé A, Sambin L, Roubille F, Andriantsitohaina R, Martinez MC and Lacampagne A. Cardioprotective effect of sonic hedgehog ligand in pig models of ischemia reperfusion. Theranostics 2020; 10: 4006-4016.

[3] Hellmann M, Piotrowski J, Kaszubowski M, Dudziak M and Anisimowicz L. Invasive assessment of the myocardial microcirculation during beating heart coronary artery bypass grafting. J Clin Med 2020; 9: 663.

[4] Zacharia E, Antonopoulos AS, Oikonomou E, Papageorgiou N, Pallantza Z, Miliou A, Mystakidi VC, Simantiris S, Kriebardis A, Orologas N, Valasiadi E, Papaioannou S, Galiatsatos N, Antoniades C and Tousoulis D. Plasma signature of apoptotic microvesicles is associated with endothelial dysfunction and plaque rupture in acute coronary syndromes. J Mol Cell Cardiol 2020; 138: 110-114.

[5] Hausenloy DJ, Chilian W, Crea F, Davidson SM, Ferdinandy P, Garcia-Dorado D, van Royen N, Schulz R and Heusch G. The coronary circulation in acute myocardial ischaemia/reperfusion injury: a target for cardioprotection. Cardiovasc Res 2019; 115: 1143-1155.

[6] Takafuji Y, Hori M, Mizuno T and Harada-Shiba M. Humoral factors secreted from adipose tissue-derived mesenchymal stem cells ameliorate atherosclerosis in Ldlr-/- mice. Cardiovasc Res 2019; 115: 1041-1051.

[7] White DA, Su Y, Kanellakis P, Kiriazis H, Morand EF, Bucala R, Dart AM, Gao XM and Du XJ. Differential roles of cardiac and leukocyte derived macrophage migration inhibitory factor in inflammatory responses and cardiac remodelling post myocardial infarction. J Mol Cell Cardiol 2014; 69: 32-42.

[8] Miyazaki Y, Kaikita K, Endo M, Horio E, Miura M, Tsujita K, Hokimoto S, Yamamuro M, Iwawaki T, Gotoh T, Ogawa H and Oike Y. C/EBP homologous protein deficiency attenuates myocardial reperfusion injury by inhibiting myocardial apoptosis and inflammation. Arterioscler Thromb Vasc Biol 2011; 31: 1124-1132.

[9] Chen Z, Chen X, Lei T, Gu Y, Gu J, Huang J, Lu B, Yuan L, Sun M and Wang Z. Integrative analysis of NSCLC identifies LINC01234 as an oncogenic lncRNA that interacts with HNRNPA2B1 and regulates miR-106b biogenesis. Mol Ther 2020; 28: 1479-1493.

[10] Ding H, Wang F, Shi X, Ma H, Du Y, Hou L and Xing N. LncRNA MALAT1 induces the dysfunction of β cells via reducing the histone acetylation of the PDX-1 promoter in type 1 diabetes. Exp Mol Pathol 2020; 114: 104432.

[11] Ou M, Zhao H, Ji G, Zhao X and Zhang Q. Long noncoding RNA MALAT1 contributes to pregnancy-induced hypertension development by enhancing oxidative stress and inflammation through the regulation of the miR-150-5p/ET-1 axis. FASEB J 2020; 345: 6070-6085.

[12] Zang X, Gu J, Zhang J, Shi H, Hou S, Xu X, Chen Y, Zhang Y, Mao F, Qian H, Zhu T, Xu W and Zhang X. Exosome-transmitted lncRNA UFC1 promotes non-small-cell lung cancer progression by EZH2-mediated epigenetic silencing of PTEN expression. Cell Death Dis 2020; 11: 215.

[13] Wu D, He X, Wang W, Hu X, Wang K and Wang M. Long noncoding RNA SNHG12 induces proliferation, migration, epithelial-mesenchymal transition and stemness of esophageal squamous cell carcinoma cells via post-transcriptional regulation of BMI1 and CTNNB1. Mol Oncol 2020; 14: 2332-2351.

[14] Chellini L, Frezza V and Paronetto MP. Dissecting the transcriptional regulatory networks of promoter-associated noncoding RNAs in development and cancer. J Exp Clin Cancer Res 2020; 39: 51.
[15] Li M, Zhang Q, Chen Y, Ren X, Gong Q and Li Y. lncRNA-PLACT1 sustains activation of NF-κB pathway through a positive feedback loop with IκBα/E2F1 axis in pancreatic cancer. Micromachines (Basel) 2020; 19: 35.
[16] Razmara E, Bitaraf A, Yousefi H, Nguyen TH, Garshasbi M, Cho WC and Babashah S. Noncoding RNAs in cartilage development: an updated review. Int J Mol Sci 2019; 20: 4475.
[17] Li T, Tian H, Li J, Zuo A, Chen J, Xu D, Guo Y and Gao H. Overexpression of lncRNA Gm2691 attenuates apoptosis and inflammatory response after myocardial infarction through PI3K/Akt signaling pathway. IUBMB Life 2019; 71: 1561-1570.
[18] Cheng Z, Zhang Q, Yin A, Feng M, Li H, Liu H, Li Y and Qian L. The long non-coding RNA uc.4 influences cell differentiation through the TGF-beta signaling pathway. Exp Mol Med 2018; 50: e447.
[19] Cheng H, Sun M, Wang ZL, Wu Q, Yao J, Ren G and Sun XL. LncRNA RMST-mediated miR-107 transcription promotes OGD-induced neuronal apoptosis via interacting with hnRNPK. Neurochem Int 2020; 133: 104644.
[20] Peng WX, Koirala P, Zhang W, Ni C, Wang Z, Yang L and Mo YY. lncRNA RMST enhances DNMT3 expression through interaction with HuR. Mol Ther 2020; 28: 9-18.
[21] Ng SY, Bogu GK, Soh BS and Stanton LW. The long noncoding RNA RMST interacts with SOX2 to regulate neurogenesis. Mol Cell 2013; 51: 349-359.
[22] Hou XX and Cheng H. Long non-coding RNA RMST silencing protects against middle cerebral artery occlusion (MCAO)-induced ischemic stroke. Biochem Biophys Res Commun 2018; 495: 2602-2608.
[23] Cao H, Fang B, Liu J, Shen Y, Shen J, Xiang P, Zhou Q, De Souza SC, Li D, Tian Y, Luo L, Zhang Z and Tian X. In vivo tracking of mesenchymal stem cell-derived extracellular vesicles improving mitochondrial function in renal ischemia-reperfusion injury. Adv Healthc Mater 2020; e2001489.
[24] Dhanesha N, Jain M, Tripathi AK, Doddapattar P, Chorawala M, Bathla G, Nayak MK, Ghatge M, Lentz SR, Kon S and Chauhan AK. Targeting myeloid-specific integrin α9β1 improves short and long-term stroke outcomes in murine models with preexisting comorbidities by limiting thrombosis and inflammation. Circ Res 2020; 126: 1779-1794.
[25] Bugger H and Pfeil K. Mitochondrial ROS in myocardial ischemia reperfusion and remodeling. Biochim Biophys Acta Mol Basis Dis 2020; 1866: 165768.
[26] Fang W, He A, Xiang MX, Lin Y, Wang Y, Li J, Yang C, Zhang X, Liu CL, Sukhova GK, Barascuk N, Larsen L, Karsdal M, Libby P and Shi GP. Cathepsin K-deficiency impairs mouse cardiac function after myocardial infarction. J Mol Cell Cardiol 2019; 127: 44-56.
[27] Zhu HH, Wang XT, Sun YH, He WK, Liang JB, Mo BH and Li L. Pim1 overexpression prevents apoptosis in cardiomyocytes after exposure to hypoxia and oxidative stress via upregulating cell autophagy. Cell Physiol Biochem 2018; 49: 2138-2150.
[28] Wei N, Chi M, Deng L and Wang G. Antioxidation role of different lateral stellate ganglion block in isoproterenol-induced acute myocardial ischemia in rats. Reg Anesth Pain Med 2017; 42: 588-599.
[29] Pan Z, Liu L, Nie W, Miggin S, Qiu F, Cao Y, Chen J, Yang B, Zhou Y, Lu J and Yang L. Long noncoding RNA AGER-1 functionally upregulates the innate immunity gene AGER and approximates its anti-tumor effect in lung cancer. Mol Carcinog 2018; 57: 305-318.
[30] Xu X, Yin Y, Tang J, Xie Y, Han Z, Zhang X, Liu Q, Qin X, Huang X and Sun B. Long non-coding RNA Myd88 promotes growth and metastasis in hepatocellular carcinoma via regulating Myd88 expression through H3K27 modification. Cell Death Dis 2017; 8: e3124.
[31] Zhang X, Dong J, Deng F, Wang W, Cheng Y, Song L, Hu M, Shen J, Xu Q and Shen F. The long non-coding RNA lncRNA973 is involved in cotton response to salt stress. BMC Plant Biol 2019; 19: 459.
[32] Zhu LY, Zhu YR, Dai DJ, Wang X and Jin HC. Epigenetic regulation of alternative splicing. Am J Cancer Res 2018; 8: 2346-2358.
[33] Ji L, Fan X, Zhou F, Gu J and Deng X. lncRNA RPL34-AS1 inhibits cell proliferation and invasion while promoting apoptosis by competitively binding miR-3663-3p/RGS4 in papillary thyroid cancer. J Cell Physiol 2020; 235: 3669-3678.
[34] Cai J, Shangguan S, Li G, Cai Y, Chen Y, Ma G, Miao Z, Liu L and Deng Y. Knockdown of lncRNA Gm11974 protect against cerebral ischemic reperfusion through miR-766-3p/NR3C2 axis. Artif Cells Nanomed Biotechnol 2019; 47: 3847-3853.
[35] Sebastiani G, Po A, Miele E, Ventriglia G, Ceccarelli E, Bugliani M, Marselli L, Marchetti P, Gulino A, Ferretti E and Dotta F. MicroRNA-124a is hyperexpressed in type 2 diabetic human pancreatic islets and negatively regulates insulin secretion. Acta Diabetol 2015; 52: 523-530.
[36] Sun S, Wang N, Sun Z, Wang X and Cui H. MiR-5692a promotes proliferation and inhibits apoptosis by targeting HOXD8 in hepatocellular carcinoma. J BUON 2019; 24: 178-186.